Asian Journal of Mechanical Engineering
ISSN: 2249-6289 (P); 3049-1886 (E)
Vol.14 No.2, 2025, pp.1-15

www.crijournals.org
DOI: https://doi.org/10.70112/arme-2025.14.2.4293

Tracking Specified Output Signals and Optimal Trajectory for Hypersonic Aircraft

Zairil A. Zaludin
Department of Aerospace Engineering, Universiti Putra Malaysia, Serdang, Selangor, Malaysia
E-mail: zairil_azhar@upm.edu.my
(Received 15 June 2025; Revised 18 July 2025; Accepted 25 August 2025; Available online 2 September 2025)

Abstract **- This article explores the intricate challenge of optimally tracking a desired trajectory within the context of hypersonic transport aircraft flight dynamics. The proposed methodology is based on Linear Quadratic Regulator (LQR) theory. An advanced tracking system is then integrated into the hypersonic aircraft closed-loop control system, utilizing a controller designed using Linear Quadratic Output Regulator (LQRY) theory. The flight dynamics of the hypersonic aircraft demonstrate the capability to track the desired output trajectory while maintaining dynamic stability. The article also includes results for tracking an optimal minimum-fuel trajectory and an optimal minimum-time trajectory. The work proposes precise speed profiles required for the aircraft to ascend to a designated altitude with optimal efficiency. The hypersonic aircraft adequately tracks both trajectories, demonstrating robustness and versatility in navigating complex flight conditions.**

Keywords: **Hypersonic Aircraft, Trajectory Tracking, Linear Quadratic Regulator (LQR), Linear Quadratic Output Regulator (LQRY), Optimal Control**

I. INTRODUCTION

It is envisioned that hypersonic vehicles will become commonplace in the future, serving various applications ranging from space exploration and long-range transportation to rapid-response military operations [1], [2]. However, to achieve this vision, optimization of aircraft flight trajectories is necessary to ensure mission success. Executing such optimization involves numerous constraints and critical factors, as discussed in [3]–[6]. These constraints include heating rates, dynamic pressure, aerodynamic loads, and the need to harmonize various re-entry tasks [7]–[9]. By formulating this challenge as an optimal control problem, trajectory optimization seeks to minimize specific objectives while rigorously adhering to essential operational requirements, thereby enhancing the safety and efficacy of hypersonic flight. Numerous studies have demonstrated that the flight dynamics of hypersonic aircraft suffer from both static and dynamic instabilities. For this reason, stability augmentation systems (SASs) have been incorporated into aircraft flight dynamics. For example, in [10], the hypersonic transport aircraft was initially found to be unstable but was successfully stabilized using LQR theory.

A control reconfiguration system based on robust LQR theory was also designed to reconfigure the optimal control system when one of the control inputs completely malfunctioned [11]. Further investigations showed that the effects of noise in the aircraft closed-loop system could be reduced using a Luenberger estimator, which requires no prior knowledge of the noise characteristics [12]. The work presented in this article proposes a methodology for optimally tracking specified trajectories based on LQR theory. The aircraft is shown to be capable of tracking the corresponding speed profiles required to reach particular altitudes while either minimizing fuel consumption or achieving those altitudes in minimum time. The remainder of this article is organized as follows. Section II introduces the description of the hypersonic aircraft. Section III presents details of the proposed methodology. Sections IV and V elaborate on the results of the simulated tests conducted. In these tests, the aircraft was subjected to commanded changes in altitude. Inspection of the model's dynamic responses was used to verify the integrity of the stable closed-loop system with the proposed engine dynamics incorporated.

A. The Vehicle

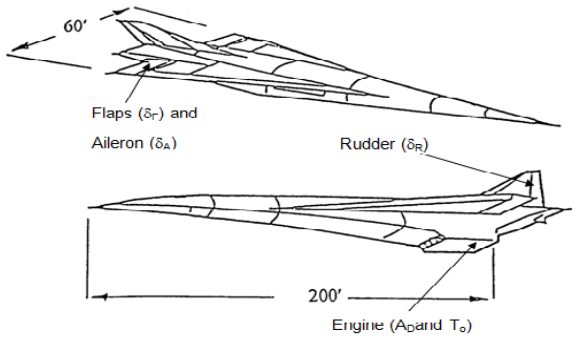

Fig.1 The Generic Hypersonic Aircraft Sketch

For convenience of reference, the name *HYPERION* is assigned to this mathematical model. A sketch of this hypothetical aircraft is shown in Figure 1. The mathematical model is linear and includes five control inputs, where δ_F denotes flap surface deflection, A_D denotes the ratio of engine diffuser area, $T_o$denotes the temperature across the engine combustor, δ_A denotes aileron deflection, and δ_R denotes rudder deflection. The *HYPERION* concept is based on the work published in [13].

II. METHODOLOGY

A. The Mathematical Model

The mathematical model is represented by a linear time-invariant state equation:

$$\dot{\boldsymbol{x}} = A\boldsymbol{x} + B\boldsymbol{u} \quad (1)$$

The state and control variables are defined in (2) and (3), respectively.

$$\boldsymbol{x} = \begin{bmatrix} \Delta u \text{ (ft/s)} \\ \Delta \alpha \text{ (rad)} \\ \Delta q \text{ (rad/s)} \\ \Delta \theta \text{ (rad)} \\ \Delta h \text{ (ft)} \\ \Delta \eta \text{ (rad)} \\ \Delta \dot{\eta} \text{ (rad/s)} \end{bmatrix} \quad (2)$$

$$\boldsymbol{u} = \begin{bmatrix} \Delta \delta_F \text{ (rad)} \\ \Delta A_D \\ \Delta T_o \ (oR) \end{bmatrix} \quad (3)$$

u, α, q, θ, h, η, $\dot{\eta}$ the bending displacement, and the rate of change of bending displacement represent the forward speed, the angle of attack, the rate of change of the pitch attitude, the pitch attitude, the altitude, the bending displacement, and the rate of change of the bending displacement, respectively. All variables are defined as perturbations about an equilibrium flight condition.

The output equation can be represented as:

$$\boldsymbol{y} = C\boldsymbol{x} + Du \quad (4)$$

where $y \in R^p$ and $u \in R^m$. The output matrix C is of order p×n and D is of order p×m. Often, not all state variables in the aircraft dynamics are measurable. For example, if only three of the seven state variables are measurable, then p=3. For the experiments discussed in this article, matrices A and B are given in (5) and (6).

$$A = \begin{bmatrix} -4.1857\times10^{-3} & -35.03 & 0.4269 & -32.2 & 7.9938\times10^{-4} & 18.614 & 0.4301 \\ -2.3158\times10^{-6} & -5.8716\times10^{-2} & 1.0002 & 0 & 4.4227\times10^{-7} & -3.9534\times10^{-2} & 2.1974\times10^{-4} \\ -9.4647\times10^{-6} & 4.3430 & -5.7885\times10^{-2} & 0 & 1.8076\times10^{-6} & 7.2990 & -5.2846\times10^{-2} \\ 0 & 0 & 1 & 0 & 0 & 0 & 0 \\ 0 & -7.8487\times10^{3} & 0 & 7.8487\times10^{3} & 0 & 0 & 0 \\ 0 & 0 & 0 & 0 & 0 & 0 & 1 \\ 1.4938\times10^{-3} & 54.953 & -0.41812 & 0 & -2.8529\times10^{-4} & -269.05 & -1.1340 \end{bmatrix} \quad (5)$$

$$B = \begin{bmatrix} -1.1359\times10^{2} & -1.7159\times10^{2} & 1.3329\times10^{-2} \\ -1.4513\times10^{-2} & 4.7726\times10^{-3} & -1.672\times10^{-7} \\ -2.3511 & -8.2859\times10^{-1} & 6.909\times10^{-5} \\ 0 & 0 & 0 \\ 0 & 0 & 0 \\ 0 & 0 & 0 \\ 0 & -9.8249\times10^{-1} & 3.4421\times10^{-5} \end{bmatrix} \quad (6)$$

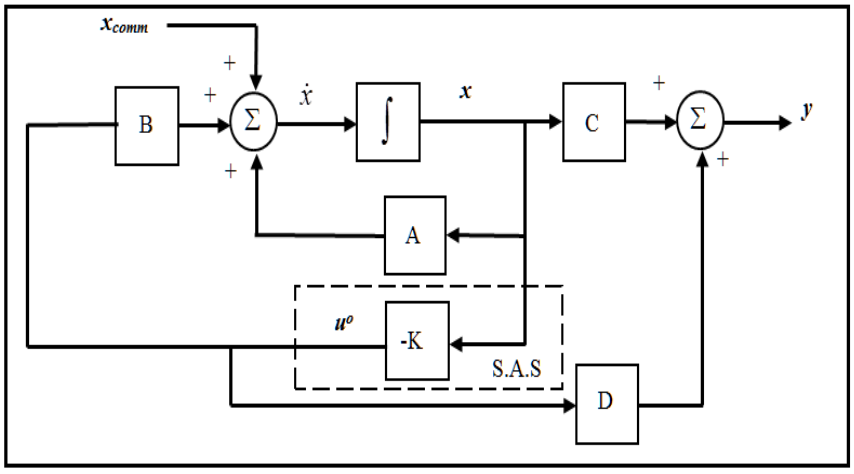

Fig.2 SAS Incorporated into Hypersonic Aircraft Flight Dynamics

B. Differences Between 'Command Input' and 'Commanded Change'

Before proceeding with the discussion of optimal tracking systems for *HYPERION*, it is useful to define two terms frequently used in this article: *command input (or signal)* and *commanded change*. A command input (or signal) is a signal that, when introduced into the aircraft dynamics, causes the aircraft to change its state from the equilibrium trimmed condition. As a result of this input, a permanent change in certain state variables from their trimmed

conditions occurs. In this article, the command signal is denoted by x_{comm}. Note that x_{comm} is a vector and is defined as follows:

$$x_{\text{comm}} = \begin{bmatrix} u_{comm} \\ \alpha_{comm} \\ q_{comm} \\ \theta_{comm} \\ h_{comm} \\ \eta_{comm} \\ \dot{\eta}_{comm} \end{bmatrix} \quad (7)$$

For these experiments, the matrices A and B of the aircraft dynamics are presented in (5) and (6). These matrices represent the aircraft flight dynamics when flying at Mach 8.0 at 85,000 ft. The first test involved the aircraft tracking a step change in altitude of 1,000 ft. It was assumed that the only measurable state variable was the change in altitude, Δh. Hence, the matrix C was defined as:

$$C = [0 \quad 0 \quad 0 \quad 0 \quad 1 \quad 0 \quad 0] \quad (8)$$

Interested readers can refer to [10] for the complete SAS design process. The SAS for the aircraft was designed using LQR theory. An appropriate command input, x_{comm}, was introduced into the aircraft dynamics to change the aircraft's altitude by the required amount. If only h_{comm} was used to command the change in altitude, the other elements in the vector of (9) were zero. Hence, the vector x_{comm} becomes:

$$x_{comm} = \begin{bmatrix} 0 \\ 0 \\ 0 \\ 0 \\ h_{comm} \\ 0 \\ 0 \end{bmatrix} \quad (9)$$

If a step command input, h_{comm}=1000, was applied, it was found that the height response of the aircraft did not settle to a steady-state value of 1,000 ft, but to 2,585.3 ft (see Figure 3).

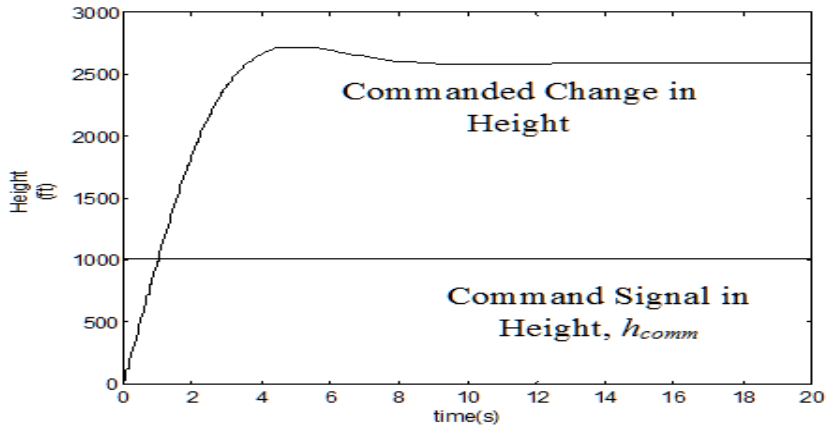

Fig.3 The Aircraft Response in Height Using Eqn (9) And h_{comm} = 1000

Clearly, the value of h_{comm} chosen did not have a one-to-one correspondence with the output variable h. Because the mathematical model of the HST is linear, the appropriate value of the command signal needed to produce a commanded change in altitude of 1,000 ft can be calculated easily once the steady-state response of the aircraft to any arbitrary command input has been determined. The term *commanded change*, in this article, is therefore defined as the steady-state change in a state variable of the aircraft resulting from a command signal introduced into the aircraft dynamics. If a steady-state altitude of 1,000 ft is required, the correct command input h_{comm} is determined using the calculation shown in Table I.

TABLE I CALCULATING h_{comm}

(Commanded Change)		**(Command Signal, h_{comm})**
2585.3ft	⇒	1000
∴1000ft	⇒	1000×1,000/2585.3 = 386.8

Because the mathematical model is linear, using h_{comm} =386.8 as the command input to the Automatic Flight Control System (AFCS) of Figure 2 resulted in achieving a height change of 1,000 ft (see Figure 4).

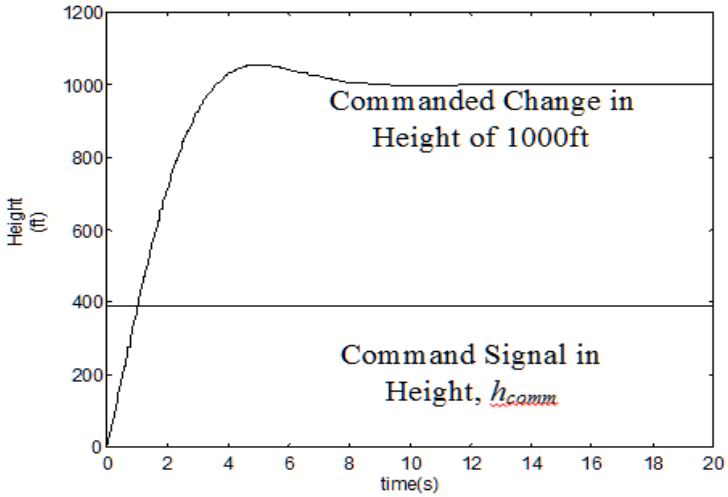

Fig.4 Commanded Change in Height of 1000ft Achieved Using h_{comm} = 386.8

This example illustrates the problem of determining the correct command input signal to track a specific output. The method discussed in the next section ensures that the step command signal matches the desired step output exactly, so that if the aircraft is required to change altitude by 1,000 ft, a step command input of h_{comm}=1000 is used.

C. Optimal Tracking System for Hyperion

In this section, the important features of an optimal tracking system are presented. A block diagram of the system integrated into the aircraft closed-loop system is shown in Figure 5. Readers can refer to [14] for an in-depth discussion of this theory. For the tracking tests, the hypersonic aircraft was stabilized using Linear Quadratic Output Regulator (LQRY) theory, which interested readers may refer to in [14]. This stabilization was necessary when applying optimal tracking theory. The matrices Q and G, used to penalize state and control actions, are shown in (10) and (11).

$$Q = [1] \tag{10}$$

$$G = \begin{bmatrix} 1 & 0 & 0 \\ 0 & 1 & 0 \\ 0 & 0 & 1 \end{bmatrix} \tag{11}$$

The values of the diagonal elements of the matrix G are unity, which implies that the control inputs $\Delta\delta_F$, ΔAD, and ΔT_o are equally penalized. Using [14], the optimal output feedback gain matrix K_y was calculated as:

$$K_y^T = \begin{bmatrix} 0 & 0.0004 & 0 \\ -704.7 & 849.9 & -0.04 \\ -1.9 & -4.4 & 0.0003 \\ 700.9 & -868.5 & 0.05 \\ 0.9 & -0.5 & 0 \\ 1.1 & -1.7 & 0 \\ 0.02 & -0.2 & 0 \end{bmatrix} \tag{12}$$

Note that although LQRY theory is used here, the control law in [14] depends on full state variable feedback, i.e., $u_o = -K_y x$.

Using (12), the eigenvalues of the aircraft closed-loop system were found to have negative real parts. These eigenvalues are presented below.

TABLE II EIGENVALUES OF THE AIRCRAFT CLOSED-LOOP SYSTEM

ζ_1	=	-0.01
$\zeta_{2,3}$	=	-0.55 ± j16.4
$\zeta_{4,5}$	=	-7.5 ± j8.1
$\zeta_{6,7}$	=	-3.9± j0.9

The optimal tracking system is stable. Next, the matrices C^TQ and $BG^{-1}B^T$ were calculated for the optimal tracking system (see Figure 5). The results of these calculations are shown below.

$$C^TQ = \begin{bmatrix} 0 \\ 0 \\ 0 \\ 0 \\ 1 \\ 0 \\ 0 \end{bmatrix} \tag{13}$$

$$BG^{-1}B^T = \begin{bmatrix} 42345.0 & 0.8 & 409.2 & 0 & 0 & 0 & 168.6 \\ 0.8 & 0 & 0.03 & 0 & 0 & 0 & -0.005 \\ 409.2 & 0.03 & 6.21 & 0 & 0 & 0 & 0.81 \\ 0 & 0 & 0 & 0 & 0 & 0 & 0 \\ 0 & 0 & 0 & 0 & 0 & 0 & 0 \\ 0 & 0 & 0 & 0 & 0 & 0 & 0 \\ 168.6 & -0.005 & 0.8 & 0 & 0 & 0 & 0.9 \end{bmatrix} \quad (14)$$

All the information required to construct the block diagram shown in Figure 5 is now available. Simulink, a dynamic simulation software package associated with MATLAB, was used to simulate the aircraft tracking a desired output. The output to be tracked was a step change in altitude of 1,000 ft; hence, z=1000 ft. When this was used as the command input, the aircraft height response was obtained and is shown in Figure 6.

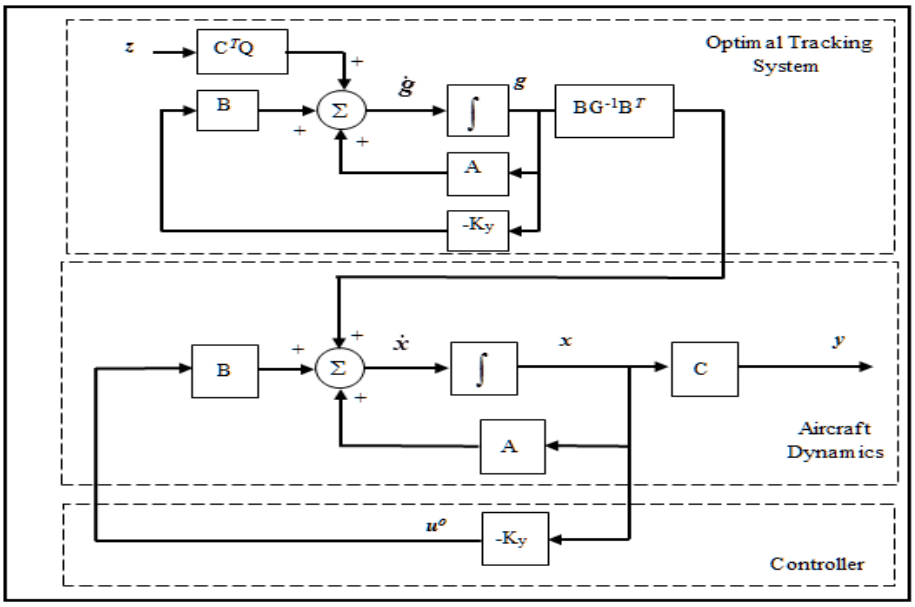

Fig.5 Optimal Closed-Loop Dynamic System with Tracking System

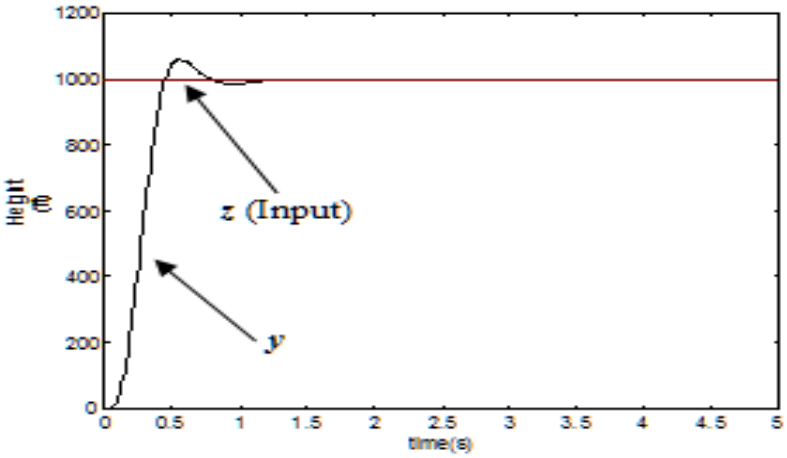

Fig.6 Height Response of Aircraft with a Tracking System

The height response showed a maximum overshoot of 60 ft, but it quickly settled to a steady value of 1,000 ft after 2 seconds. Similar results were obtained when the aircraft was tested to track different step outputs. These tests demonstrate that the aircraft can successfully track any desired step output. The aircraft system was then tested to evaluate its response to a ramp change in altitude. The aircraft's closed-loop system was required to increase altitude linearly by 1,000 ft in 10 seconds. Therefore, the slope of the ramp input was 100. Using the same closed-loop aircraft configuration with the optimal tracking system as before, this ramp input was introduced as the command input to the aircraft dynamics. The resulting aircraft response is shown in Figure 7.

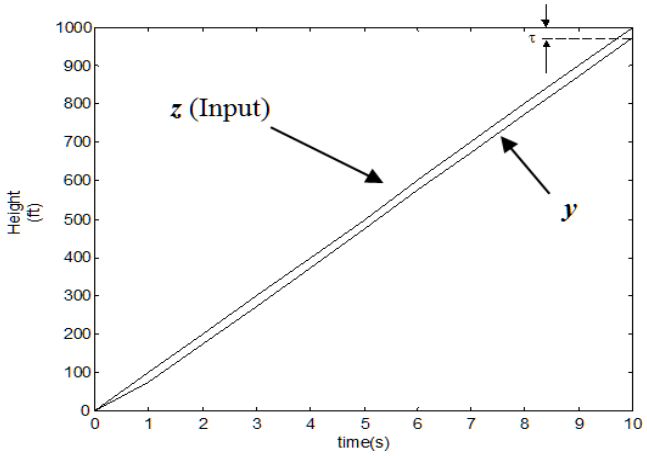

Fig.7 The Aircraft Tracking a Ramp Command Input in Height

It can be seen that the aircraft response lags behind the commanded change. Figure 7 shows that the aircraft response lags behind the command input by a constant value, namely, τ=25 ft. It is of interest to examine the aircraft response when the forcing factor $\dot{g}$ in (14) is set to zero, which occurs when g is constant. When $\dot{g}=0$, the vector g becomes a function of the desired output vector z, i.e.

$$g = \left[\left[\mathrm{A} - \mathrm{BG}^{-1}\mathrm{B}^{T}\hat{\mathrm{P}}\right]^{T}\right]^{-1}[\mathrm{C}^{T}\mathrm{Q}].z \tag{15}$$

The block diagram of the aircraft closed-loop system with the modified tracking system is shown in Figure 9. The responses of the controlled aircraft with the tracking system for $\dot{g}\neq 0$ and $\dot{g}=0$ can now be compared. In both cases, the aircraft was commanded to track a step change in altitude of 1,000 ft. The resulting responses are presented in Figure 8.

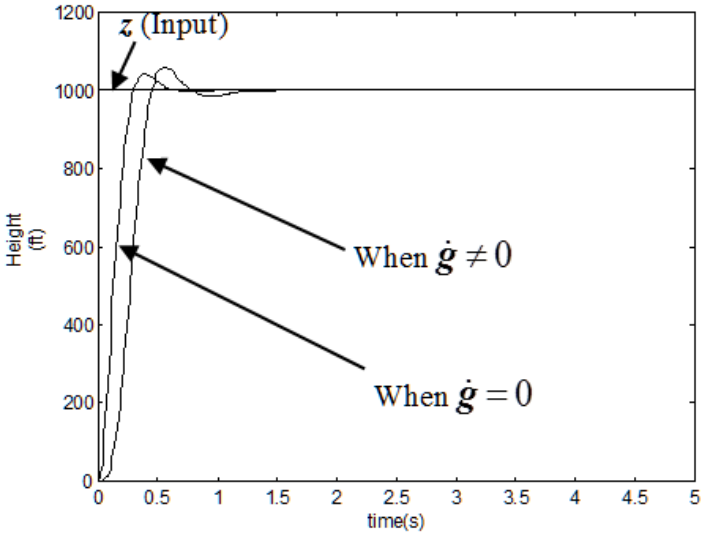

Fig.8 The Response from the Aircraft with $\dot{g} \neq 0$ and $\dot{g} = 0$

The aircraft that assumed $\dot{g}=0$ was still able to track the step change in altitude, reaching its maximum peak earlier (t=0.5 s) than the aircraft that assumed $\dot{g}\neq 0$. The response of the second aircraft was almost completely settled at the same time as that of the first aircraft, i.e., at t=2 s.

III. RESULTS FROM TRACKING MINIMUM FUEL TRAJECTORY TEST

It is assumed that the HST will be used to transport passengers and cargo between continents. One of the key requirements for such a vehicle is the ability to carry the maximum possible payload, i.e., the payload should be maximized. Consequently, the amount of fuel that can be carried on-board will be limited. Hence, fuel usage must be optimized by flying an appropriate optimal trajectory. A minimum-fuel trajectory for a similar HST has been proposed and published in [15]. The trajectory was calculated using the energy-state method and consists of velocity profiles at which the aircraft should fly to reach the desired altitude while consuming a minimum amount of fuel. However, this trajectory was developed for an HST mission involving payload insertion into low Earth orbit, rather than passenger transport between continents. This trajectory, known as the Schmidt–Hermann trajectory, is shown below for reference.

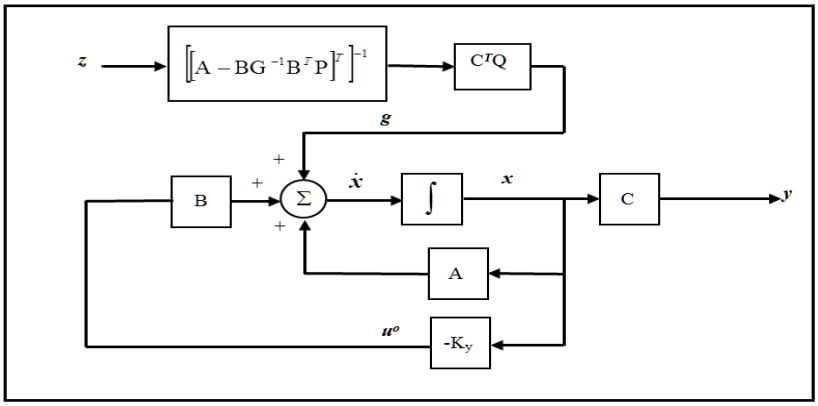

Fig.9 When $\dot{g} = 0$

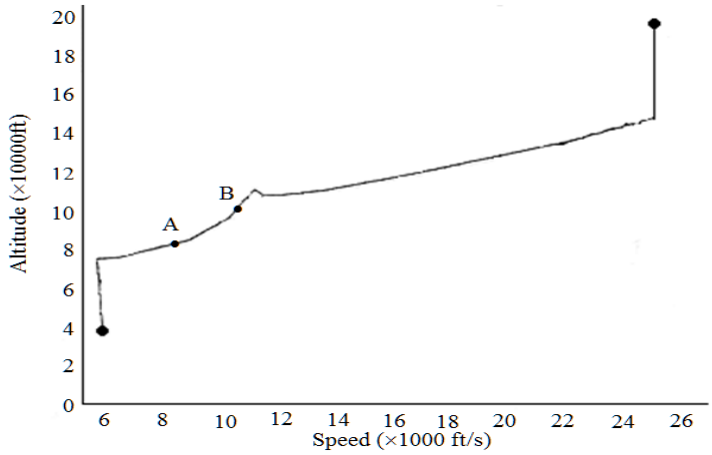

Fig.10 Minimum Fuel Trajectory [15]

All the work involved in this research centered on the scramjet-powered phase of the HST flight. It is expected that the scramjet-powered phase would be initiated only after the vehicle is first accelerated using a more conventional means of propulsion, such as a turbo-ramjet [16]. Hyperion was expected to fly at altitudes between 85,000 ft and 100,000 ft during this phase. In Figure 10, the speed trajectories corresponding to these altitudes are marked A and B. It can be seen that these trajectories are close to linear (See Figure 11).

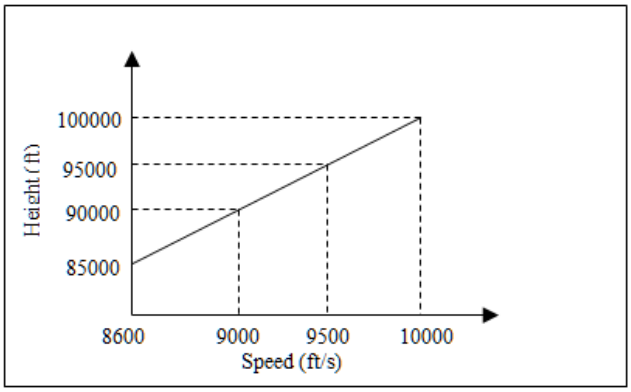

Fig.11 Minimum Fuel Trajectory for Hyperion Flying Between 85000 – 100000ft

The Schmidt–Hermann trajectory did not include the times required to reach the appropriate altitude destinations while flying at the recommended speeds. The calculation of the times needed for Hyperion to reach its altitude destinations using the specified speeds is presented in the following section. The mathematical model considered in this article corresponds to the aircraft flying at 7,848.7 ft/s (Mach 8.0) at an altitude of 85,000 ft. From Figure 10, it can be seen that, when flying at this altitude, the aircraft should be flying at 8,600 ft/s. Therefore, the aircraft speed needs to be

increased by 751.3 ft/s. To increase the speed to the required value, a commanded step change in speed of 751.3 ft/s was initiated for the test.

Once the aircraft reached this speed while maintaining altitude, the first change in altitude was from 85,000 ft to 90,000 ft, and the aircraft speed was required to increase from 8,600 ft/s to 9,000 ft/s. The time taken to fly from 85,000 ft to 95,000 ft was:

$$\frac{\partial h}{\partial u} = \frac{90000-85000}{9000-8600} = \frac{5000}{400} = 12.5\text{seconds} \quad (16)$$

Hence, the aircraft had to increase its altitude from 85,000 ft to 90,000 ft and change its speed from 8,600 ft/s to 9,000 ft/s in 12.5 s.

The next climb in altitude was from 90,000 ft to 95,000 ft. To accomplish this, the aircraft had to increase its speed from 9,000 ft/s to 9,500 ft/s. The time taken to do this is therefore,

$$\frac{\partial h}{\partial u} = \frac{95000-90000}{9500-9000} = \frac{5000}{500} = 10.0\text{seconds} \quad (17)$$

Finally, the aircraft reached 100,000 ft from 95,000 ft, flying at speeds increasing from 9,500 ft/s to 10,000 ft/s. The time taken for this part of the trajectory was:

$$\frac{\partial h}{\partial u} = \frac{100000-95000}{10000-9500} = \frac{5000}{500} = 10.0\text{second} \quad (18)$$

Using a minimum-fuel trajectory, the total time taken to fly from 85,000 ft to 100,000 ft was therefore:

$$12.5 + 10.0 + 10.0 = 32.5 \text{ seconds.} \quad (19)$$

The height and speed trajectories that the aircraft must follow to achieve the minimum-fuel trajectory are shown in the following figures.

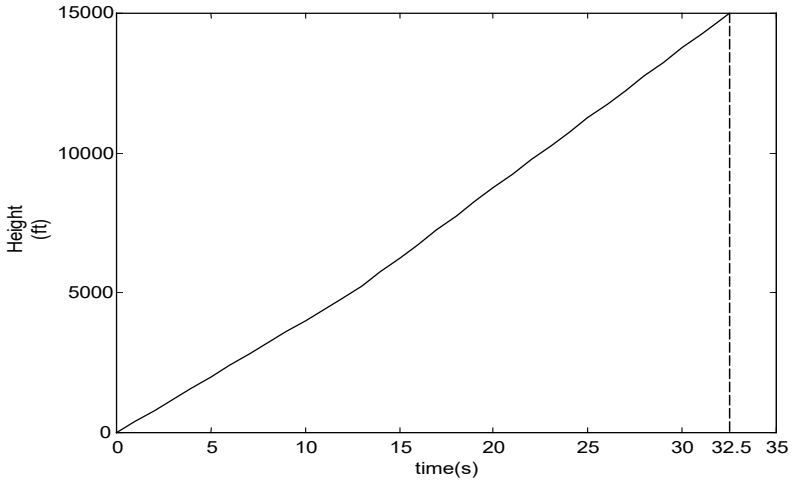

Fig.12 Height Trajectory for Aircraft to Achieve the Minimum Fuel Trajectory

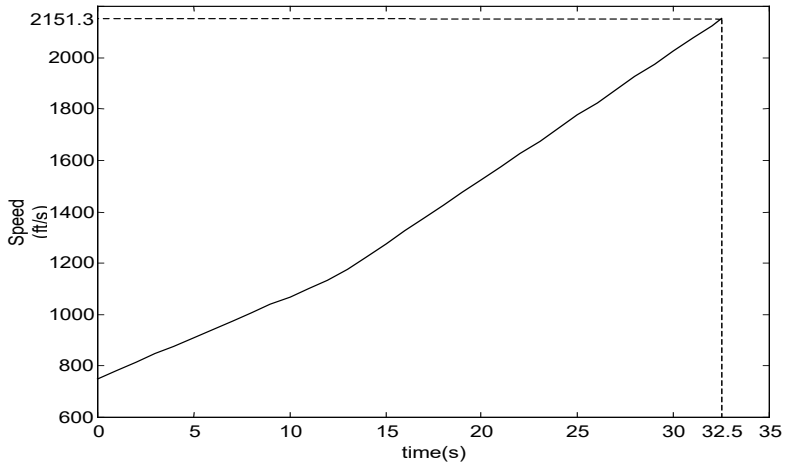

Fig.13 Speed Trajectory for Aircraft to Achieve the Minimum Fuel Trajectory

These altitude and speed trajectories were used as the command input, z, for the AFCS with a tracking system. For this work, g˙=0 was assumed; hence, the tracking system shown in Figure 9 was used to track the specified trajectory.

The altitude and speed responses of the closed-loop aircraft with the tracking system, using the minimum-fuel trajectories of Figure 12 and Figure 13, are shown in Figure 14 and Figure 15, respectively.

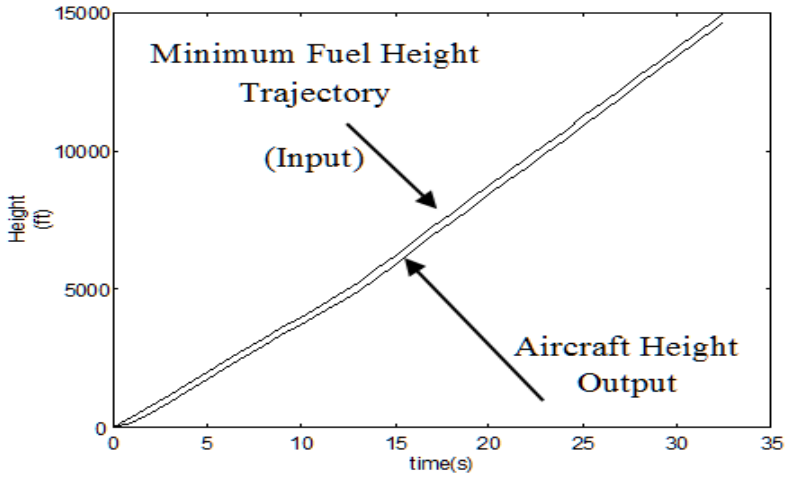

Fig.14 Hyperion Tracking Height Trajectory to Achieve Minimum Fuel Trajectory

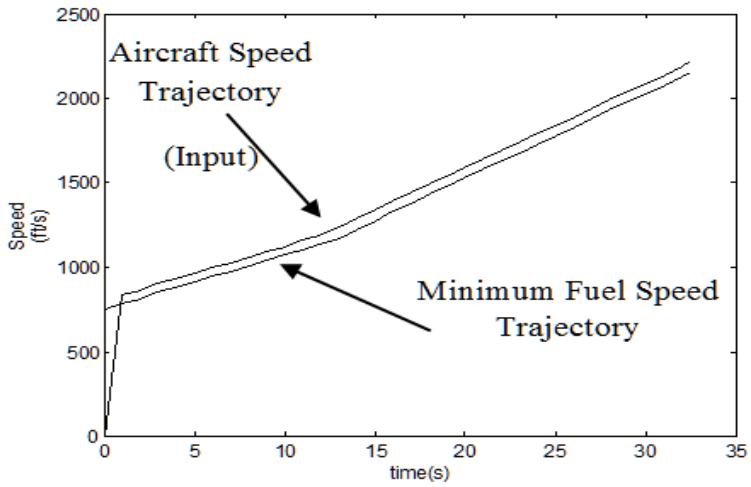

Fig.15 Hyperion Tracking Speed Trajectory to Reach 100000ft to Achieve Minimum Fuel Trajectory

Note that the aircraft was tracking ramp inputs until it reached a final altitude of 100,000 ft and a speed of 10,000 ft/s. It can be seen that, when the input reached the final destinations, the aircraft response lagged behind the input by 333.3 ft and 58.8 ft/s, respectively. This indicates that the aircraft did not reach its final altitude and speed at 32.5 s. To overcome this deficiency, it was found necessary to hold the final altitude and speed commands for 2 s to allow the aircraft dynamics to catch up with the command inputs. The aircraft responses using the extended input are shown below.

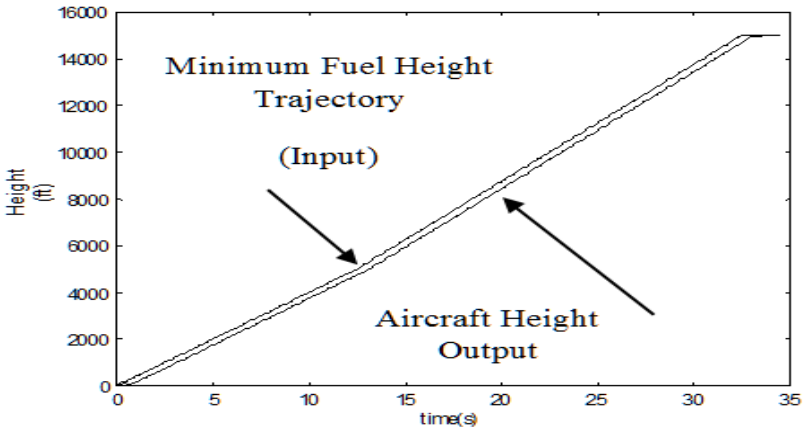

Fig.16 The Aircraft Finally Reaches the Final Height Specified By the Trajectory

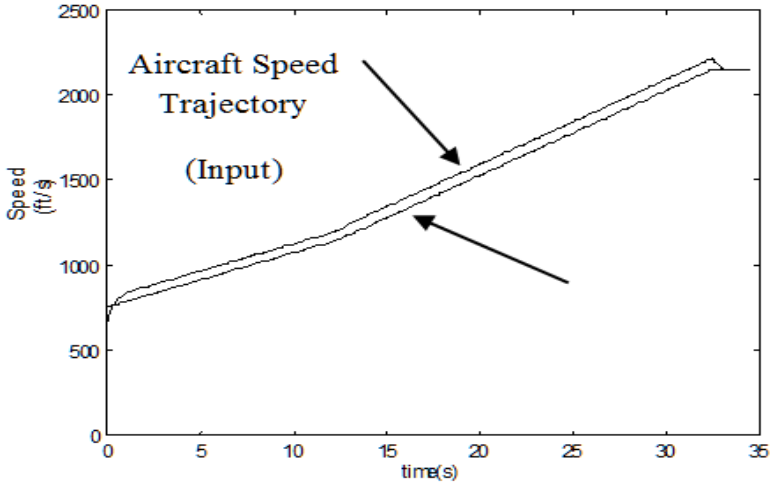

Fig.17 The Aircraft Finally Reached the Final Speed Specified By the Trajectory

Both the altitude and speed responses indicate that the aircraft's optimal tracking system was able to track the minimum-fuel trajectory. The behavior of the other state variables of the aircraft, such as angle of attack and pitch rate, during these trajectories was also examined and is plotted in Figure 18 and Figure 19.

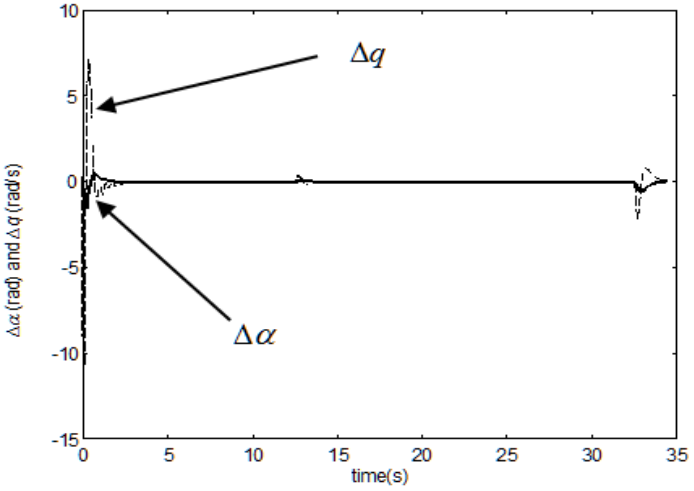

Fig.18 $\Delta\alpha$ and Δq Responses

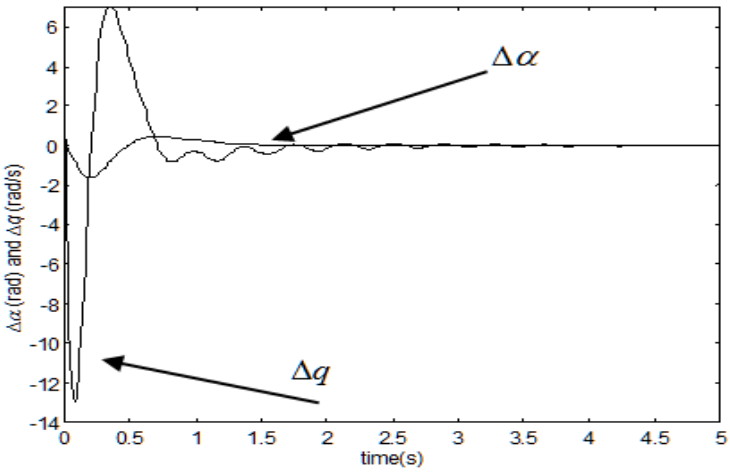

Fig.19 The Same Response Shown in Fig.18 But Only in the First 5 Seconds

In deriving the mathematical model [17], Hyperion, flying at Mach 8.0 and at an altitude of 85,000 ft, had its angle of attack, α, trimmed at −0.03 rad (−2.0°). However, the pitch rate, q, was not trimmed. When the command input was fed into the AFCS to track the minimum-fuel trajectory, greater activity was observed in the change in pitch rate, Δq, than in the change in angle of attack, Δα. Recall that the first command input applied was a step change in speed of 751.3 ft/s, while no commanded change in altitude was applied. Δq immediately peaked at −13.0 rad/s in response to this change, while, on the other hand, the angle of attack immediately decreased from its trimmed value by 1.6 rad. Immediately afterward, the pitch-rate response changed to 7.0 rad/s, followed by the small oscillations shown in Figure 19. These oscillations had a frequency of approximately 2 Hz with a damping ratio of 0.7 and settled after approximately 7 s. Δα, however, exhibited one cycle of oscillation before settling to zero.

The next instance at which activity was recorded in Δq and Δα occurred at 12.5 s, as shown in Figure 18. At this time, the second change in the commanded altitude and speed was initiated. The changes in these state variables peaked at 0.4 rad/s for Δq and 0.8 rad for Δα. Further changes were also observed at 32.5 s, when the final command input was applied to the AFCS. At this time, Δα decreased by 0.56 rad, while Δq decreased by 2.3 rad/s. The angle of attack then exhibited a positive increase and settled to its new trimmed value at 34.5 s. The pitch rate also increased, peaking at 0.8 rad/s, before settling to zero at 34.5 s. From these responses, it is evident that changes in angle of attack and pitch attitude occurred only when command inputs were applied to the AFCS. The largest activities occurred when a commanded change in speed was applied at the start of the tracking maneuver, where the speed command could be considered relatively abrupt. When no abrupt changes in command input occurred, no significant activity in either angle of attack or pitch rate was observed.

IV. RESULTS FROM TRACKING MINIMUM TIME TRAJECTORY TEST

In this section, the results of using the trajectory that minimizes the time to reach altitude as an input to the AFCS are presented. These data were also obtained from [15], and, as before, the trajectory corresponds to an HST delivering its payload to low Earth orbit. The minimum-time trajectory is shown below for convenience.

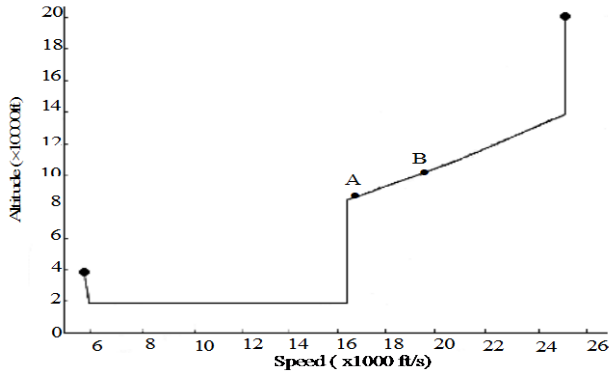

Fig.20 Minimum Time Trajectory

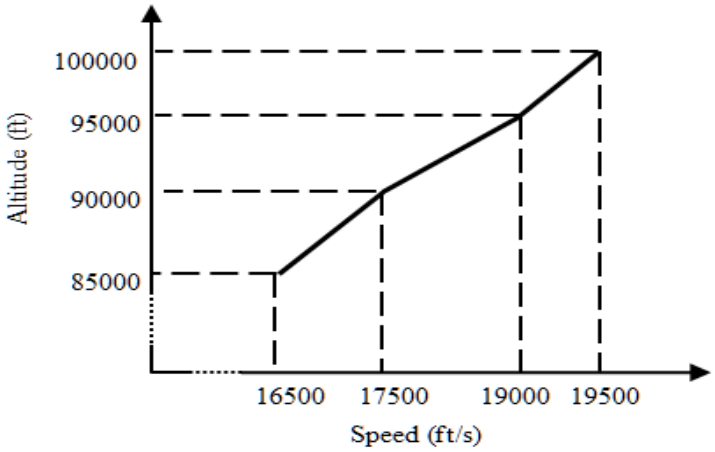

Fig.21 Minimum Time Trajectory for Hyperion Flying Between 85000ft and 100000ft

The times taken to reach the altitudes and speeds indicated at points A and B in Figure 20 are determined next. From Figure 20, it can be seen that the aircraft should be flying at a speed of 16,500 ft/s when at an altitude of 85,000 ft. As

mentioned previously, the mathematical model corresponds to the HST initially flying at Mach 8.0 (7,848.7 ft/s) at this altitude. Thus, the aircraft speed must be increased by 8,651.3 ft/s. In terms of Mach number, the aircraft's Mach number must be increased from 8.0 to 16.8, more than double its trimmed value. In the first instance, a commanded step change in speed to Mach 16.8 (16,500 ft/s) was initiated for Hyperion, which was flying at its trimmed speed of Mach 8.0 (7,848.7 ft/s). This represents a significant increase in speed over a short period of time. However, this article is primarily concerned with the tracking ability of the HST and the behavior of the state variables while tracking a specified trajectory. Little consideration is given at this stage to flying quality issues. Nevertheless, later in this article, it is shown that, instead of dramatically increasing the speed using a step command input, a smoothed command, implemented via a first-order filter, was used to increase the speed to Mach 16.8. The next altitude change was to 90,000 ft. To climb to this altitude, the aircraft's speed had to be increased to 17,500 ft/s. The time taken to climb from 85,000 ft to 95,000 ft was calculated next.

$$\frac{\partial h}{\partial u} = \frac{90000-85000}{17500-16500} = \frac{5000}{1000} = 5.0\text{seconds} \quad (20)$$

Hence, the aircraft had to increase its altitude from 85,000 ft to 90,000 ft and its speed from 16,500 ft/s to 17,500 ft/s in 5 s. Note that the time taken to climb to this altitude was different from that of the minimum-fuel trajectory, which was 12.5 s. The next climb in altitude was to 95,000 ft. To achieve this, the aircraft speed was increased from 17,500 ft/s to 19,000 ft/s. The time taken to do so was calculated as:

$$\frac{\partial h}{\partial u} = \frac{95000-90000}{19000-17500} = \frac{5000}{1500} = 3.33\text{seconds} \quad (21)$$

Finally, the aircraft reached the target altitude of 100,000 ft from 95,000 ft by smoothly increasing its speed from 19,000 ft/s to 19,500 ft/s. The time taken for this part of the trajectory was:

$$\frac{\partial h}{\partial u} = \frac{100000-95000}{19500-19000} = \frac{5000}{500} = 10.0\text{second} \quad (22)$$

The total time taken to fly from 85,000 ft to 100,000 ft using the minimum-time trajectory was calculated to be:

$$5.0 + 3.33 + 10.0 = 18.33 \text{ seconds.} \quad (23)$$

To achieve the minimum-time trajectory, the aircraft had to accurately follow the altitude and speed trajectories shown in Figure 22 and Figure 23.

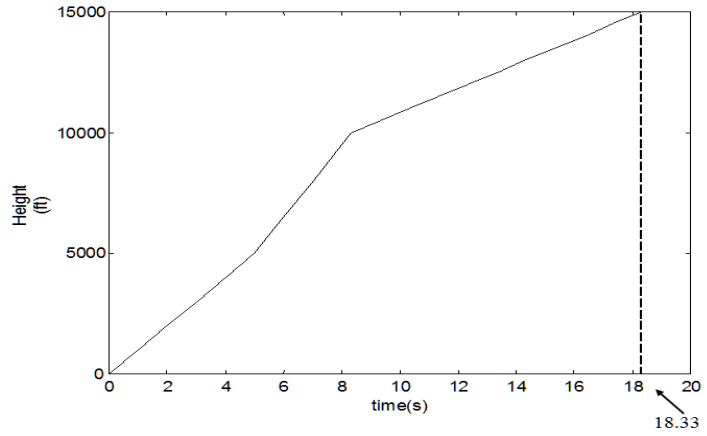

Fig.22 Height Trajectory for Minimum Time

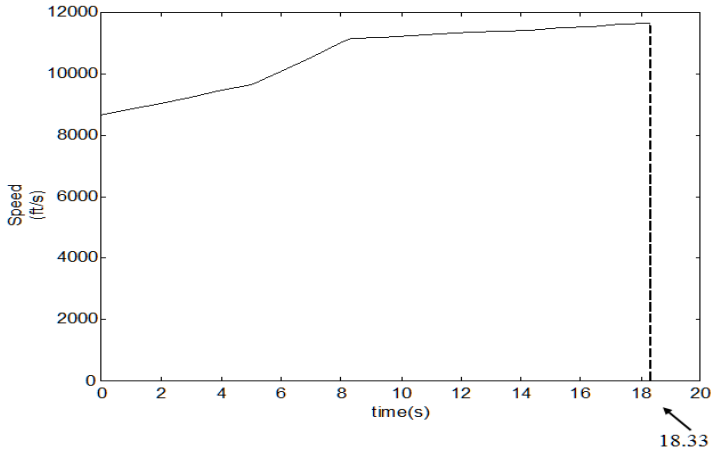

Fig.23 Speed Trajectory for Minimum Time

Using these trajectories as command inputs to the HST's tracking system, the aircraft effectively tracked the commands, as shown in Figures 24 and 25. Additionally, ramp inputs were used to monitor the trajectory's final altitude and speed. The aircraft responses lagged behind the inputs. To eliminate the resulting error, it was necessary to maintain both the altitude and speed command signals for an additional 2 s at 100,000 ft and 19,500 ft/s. The aircraft responses to these commanded inputs are shown in Figure 26 and 27.

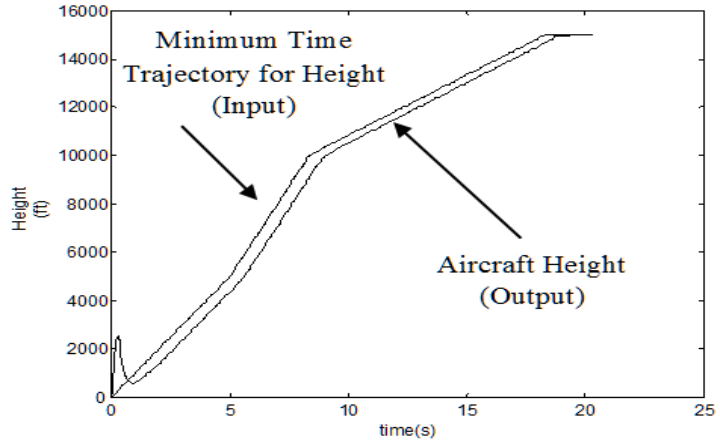

Fig.24 Tracking Height Using Minimum Time Trajectory

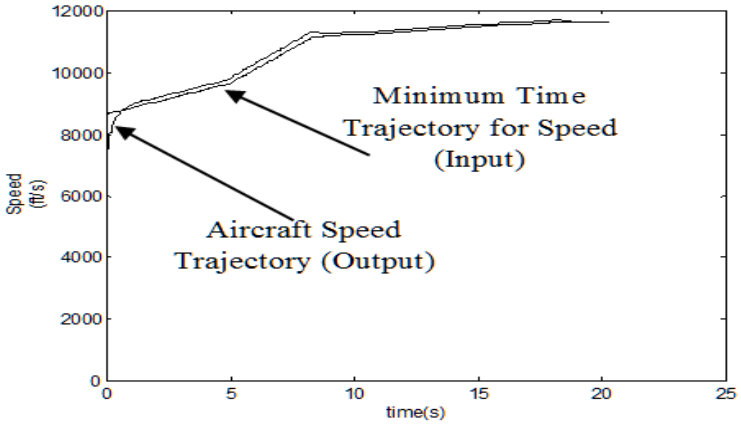

Fig.25 Tracking Speed Using Minimum Time Trajectory

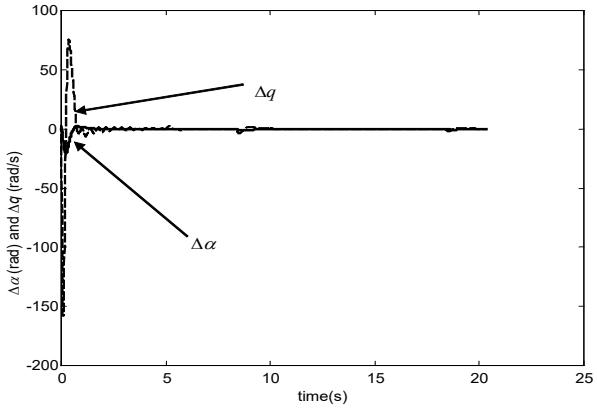

Fig.26 $\Delta\alpha$ and Δq responses

In the first second, an overshoot in altitude was observed as the aircraft attempted to track the significant change in speed. The overshoot peaked at 2,530.6 ft. Even though a significant commanded change in speed was input into the AFCS, the aircraft dynamics were still able to track the desired change. The effect on the aircraft when tracking the first commanded step change in speed can be observed more clearly by examining the pitch rate and angle of attack

responses. A sudden decrease in pitch rate to –160 rad/s and in angle of attack by –21 rad is shown by the aircraft dynamics. The angle of attack quickly settled after approximately 3 seconds, but the pitch rate increased sharply shortly afterward to 75 rad/s. The pitch rate response displayed small oscillations (see Figure 27), but before it could settle, a new commanded change in altitude and speed occurred at 5 seconds. The new command input caused a maximum change in pitch rate of 2.2 rad, which is relatively small compared to the response resulting from the first command input. Small changes in state variables were observed during the remainder of the trajectory before reaching a height of 100,000 ft.

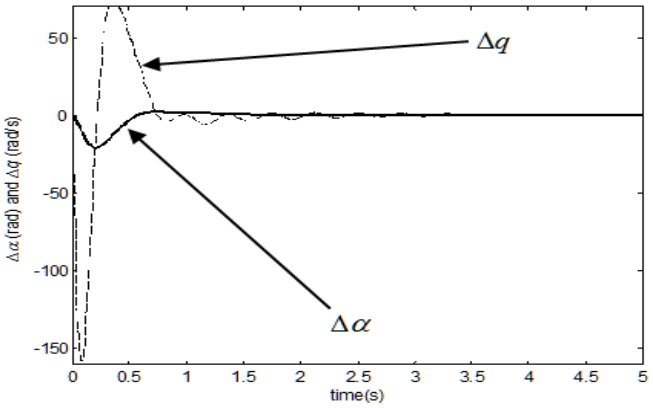

Fig.27 The Same Response Shown in Fig.26 But Only in the First 5 Seconds After the AFCS was Fed with the Commanded Input

If it is assumed that the aircraft speed was increased gradually from Mach 8.0 (7,848.7 ft/s) to Mach 16.8 (16,500 ft/s) using a first-order filter, the question arises as to whether the aircraft pitch rate and pitch attitude would result in a smaller change. The speed of the aircraft was increased from Mach 8.0 to Mach 16.8 using a first-order linear filter with a time constant of 1 second. As before, the aircraft was able to track the height and speed trajectories successfully. The corresponding angle of attack and pitch rates are shown in Figure 26.

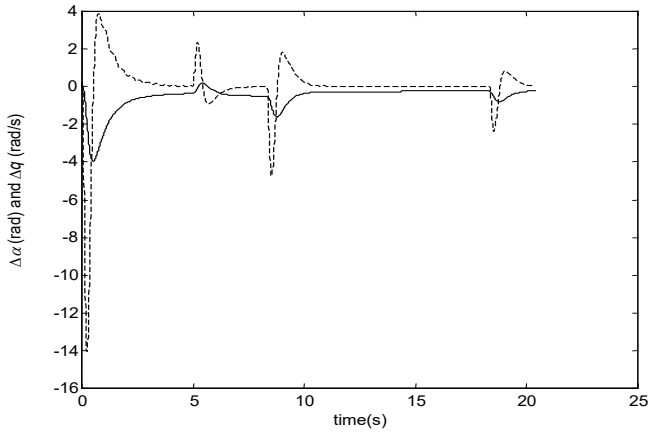

Fig.28 Pitch Rate and Angle of Attack Responses When Using a First-Order Filter to Change Speed from Mach 8.0 to Mach 16.8 Instead of Using a Step-Input.

The sudden change in pitch rate observed in the first few seconds of Figure 26 was still visible, albeit less pronounced than before, as shown in Figure 28. Consequently, the gradual increase in speed using the filter resulted in a subtle change in the angle of attack.

V. CONCLUSION

In this article, the problem of optimally tracking a desired trajectory was addressed. The theory was based on LQR. The tracking system was then integrated into the Hyperion closed-loop control system with a controller designed using LQRY. When the aircraft was subjected to a command input, the closed-loop system with the optimal tracking system was found to be dynamically stable and capable of tracking the desired output. The article demonstrated that the aircraft was able to track either a minimum-fuel trajectory or a minimum-time trajectory. The trajectories specified the speeds at which the aircraft should fly to reach a specified altitude. Hyperion successfully tracked both minimum-fuel and minimum-time trajectories.

Declaration of Conflicting Interests
The author declares no potential conflicts of interest with respect to the research, authorship, and/or publication of this article.

Funding
The author received no financial support for the research, authorship, and/or publication of this article.

Use of Artificial Intelligence (AI)-Assisted Technology for Manuscript Preparation
The author confirms that no AI-assisted technologies were used in the preparation or writing of the manuscript, and no images were altered using AI.

ORCID
Zairil A. Zaludin https://orcid.org/0000-0001-9599-4084

REFERENCES

[1] Y. Ding, X. Yue, G. Chen, and J. Si, "Review of control and guidance technology on hypersonic vehicle," *Chinese J. Aeronaut.*, vol. 35, no. 7, pp. 1–18, 2022, doi: 10.1016/j.cja.2021.10.037 .

[2] J. Zhao and R. Zhou, "Reentry trajectory optimization for hypersonic vehicle satisfying complex constraints," *Chinese J. Aeronaut.*, vol. 26, no. 6, pp. 1544–1553, 2013, doi: 10.1016/j.cja.2013.10.009.

[3] G. Kumar, D. Penchalaiah, A. Sarkar, and S. Taloe, "Hypersonic boost-glide vehicle trajectory optimization using genetic algorithm," *IFAC-PapersOnLine*, vol. 51, no. 1, pp. 118–123, 2018, doi: 10.1016/j.ifacol.2018.05.020.

[4] Y. Ma, B. Pan, C. Hao, and S. Tang, "Improved sequential convex programming using modified Chebyshev–Picard iteration for ascent trajectory optimization," *Aerospace Sci. Technol.*, vol. 120, Art. no. 107234, 2022, doi: 10.1016/j.ast.2021.107234.

[5] L. Pan, S. Peng, Y. Xie, Y. Liu, and J. Wang, "3D guidance for hypersonic reentry gliders based on analytical prediction," *Acta Astronaut.*, vol. 167, pp. 42–51, 2020, doi: 10.1016/j.actaastro.2019.07.039.

[6] B. Zhang, S. Tang, and B. Pan, "Multi-constrained suboptimal powered descent guidance for lunar pinpoint soft landing," *Aerospace Sci. Technol.*, vol. 48, pp. 203–213, 2016, doi: 10.1016/j.ast.2015.11.018.

[7] R. Chai, A. Tsourdos, A. Savvaris, S. Chai, and Y. Xia, "Trajectory planning for hypersonic reentry vehicle satisfying deterministic and probabilistic constraints," *Acta Astronaut.*, vol. 177, pp. 30–38, 2020, doi: 10.1016/j.actaastro.2020.06.051.

[8] T. Zhang, H. Su, and C. Gong, "hp-adaptive RPD based sequential convex programming for reentry trajectory optimization," *Aerospace Sci. Technol.*, vol. 130, Art. no. 107887, 2022, doi: 10.1016/j.ast.2022.107887.

[9] H. Zhou, X. Wang, and N. Cui, "Glide trajectory optimization for hypersonic vehicles via dynamic pressure control," *Acta Astronaut.*, vol. 164, pp. 376–386, 2019, doi: 10.1016/j.actaastro.2019.08.012.

[10] D. McLean and Z. Zaludin, "Stabilization of longitudinal motion of a hypersonic transport aircraft," *Trans. Inst. Meas. Control*, vol. 21, no. 2–3, pp. 99–105, 1999, doi: 10.1177/014233129902100206.

[11] Z. A. Zaludin, "Regaining loss in dynamic stability after control surface failure for an air-breathing hypersonic aircraft flying at Mach 8.0," *Asian Rev. Mech. Eng.*, vol. 10, no. 2, pp. 1–9, 2021, doi: 10.51983/arme-2021.10.1.2961.

[12] Z. A. Zaludin, "Sensor and process noises reduction using a Luenberger state estimator with a stability augmentation system for a hypersonic transport aircraft," *Asian Rev. Mech. Eng.*, vol. 11, no. 1, pp. 40–52, 2022, doi: 10.51983/arme-2022.11.1.3346.

[13] F. Chavez and D. Schmidt, "Analytical aeropropulsive/aeroelastic hypersonic-vehicle model with dynamic analysis," *J. Guid. Control Dyn.*, vol. 17, no. 6, pp. 1308–1319, 1994, doi: 10.2514/3.21349.

[14] M. Athans and P. L. Falb, "The design of optimal linear systems with quadratic criteria," in *Optimal Control – An Introduction to the Theory and Its Applications*, New York, NY, USA: McGraw-Hill, 1966.

[15] D. Schmidt and J. Hermann, "Use of energy-state analysis on a generic air-breathing hypersonic vehicle," *J. Guid. Control Dyn.*, vol. 21, no. 1, pp. 71–76, 1998.

[16] D. Schmidt, "Mission performance, guidance and control of a generic air-breathing launch vehicle," *Adv. Astronaut. Sci.*, vol. 92, Art. no. AAS 96-023, pp. 243–262, 1996.

[17] Z. A. Zaludin, "Mathematical model of an aircraft flying over a range of hypersonic speeds and heights," Aeronautics and Astronautics Department, Southampton University, Tech. Rep. AASU 98/01, 1998.